

Impurities near an Antiferromagnetic-Singlet Quantum Critical Point

T. Mendes^{1,2}, N. Costa¹, G. Batrouni^{3,4,5,6}, N. Curro², R.R. dos Santos¹, T. Paiva¹, and R.T. Scalettar²

¹*Instituto de Física, Universidade Federal do Rio de Janeiro Cx.P. 68.528, 21941-972 Rio de Janeiro RJ, Brazil*

²*Physics Department, University of California, Davis, California 95616, USA*

³*Université Côte d'Azur, INLN, CNRS, France*

⁴*Institut Universitaire de France, 75005 Paris, France*

⁵*MajuLab, CNRS-UNS-NUS-NTU International Joint Research Unit UMI 3654, Singapore and*

⁶*Centre for Quantum Technologies, National University of Singapore; 2 Science Drive 3 Singapore 117542*

Heavy fermion systems, and other strongly correlated electron materials, often exhibit a competition between antiferromagnetic (AF) and singlet ground states. Using exact Quantum Monte Carlo (QMC) simulations, we examine the effect of impurities in the vicinity of such AF-singlet quantum critical points, through an appropriately defined “impurity susceptibility,” χ_{imp} . Our key finding is a connection, within a single calculational framework, between AF domains induced on the singlet side of the transition, and the behavior of the nuclear magnetic resonance (NMR) relaxation rate $1/T_1$. We show that local NMR measurements provide a diagnostic for the location of the QCP which agrees remarkably well with the vanishing of the AF order parameter and large values of χ_{imp} . We connect our results with experiments on Cd-doped CeCoIn₅.

PACS numbers: 71.10.Fd, 71.30.+h, 02.70.Uu

Introduction: In materials like the cuprate superconductors, mobile impurities, introduced *e.g.* via the replacement of La by Sr, are known to destroy antiferromagnetic (AF) order very rapidly^{1,2}. Long range spin correlations are somewhat more robust to static scatterers, *e.g.* via Zn substitution for Cu in the same materials^{3–5}. This competition of AF and chemical doping is a central feature of many other strongly correlated systems, including Li doping in nickel oxides^{6,7}, spin chains⁸, and ladders⁹, and has been explored by QMC approaches in single band fermion models¹⁰ and their strong coupling spin limits¹¹.

Materials with multiple fermionic bands or localized spins in multi-chain or multi-layer geometries offer an additional richness to the problem of the effect of impurities on AF, since even in the clean limit they can exhibit a quantum critical point (QCP) separating AF and singlet phases. Disorder introduces a non-trivial effect on this transition: Although impurities reduce AF deep in the ordered phase, nearer to the QCP they can increase AF and even, beginning in the quantum disordered phase, *induce* AF by breaking singlets^{8,9}.

This effect has recently been explored in heavy-fermion materials where, *e.g.* Cd doping of superconducting CeCoIn₅ induces long range magnetic order¹². The underlying mechanism is believed to be a local reduction of conduction electron-local moment hybridization on the Cd sites, suppressing the energy gain of singlet formation. The size of these AF regions shrinks with the application of pressure, which increases this hybridization towards its value in the absence of disorder, ultimately yielding a revival of superconductivity (SC). However, the resulting phase is quite heterogeneous¹³, not unlike the stripe and nematic orders which coexist with superconductivity in the cuprates. Prior theoretical work examined domains within the context of a mean field theory (MFT) treatment of competing AF and SC orders¹³.

In this paper, we report QMC simulations of a disordered bilayer Heisenberg Hamiltonian, and characterize its physics within an exact treatment of quantum many body fluctuations. Our key findings are: (i) An appropriately defined impurity susceptibility captures both the inhibition of AF order deep in the ordered phase, and its sharp enhancement near the QCP; (ii) Quantitative determination of the AF regions induced by impurities, and the criterion for their coalescence into a state with long range order at experimentally relevant temperature scales; (iii) Verification of the suggestion that the NMR relaxation rate is temperature-independent at the QCP, and the demonstration that the local value of $1/T_1$ on an impurity site increases abruptly.

QMC, in combination with analytic scaling arguments, has previously been used to study the loss of magnetic order and multicritical points in bilayers where the dilution at a given site discards simultaneously the spins in *both* layers¹⁸. Interesting topological considerations arise from the removal of a *single* spin from a bilayer system in the singlet phase, since an unpaired spin-1/2 object is left behind¹⁹. QMC has been used to study the spin texture produced by a single impurity²⁰ as well as the onset of AF order in lattices of dimerized chains²¹.

Model and Methods:

We consider the AF Heisenberg bilayer Hamiltonian

$$H = \sum_{\langle ij \rangle, \alpha} J^\alpha \vec{S}_i^\alpha \cdot \vec{S}_j^\alpha + g \sum_i \vec{S}_i^1 \cdot \vec{S}_i^2 \quad (1)$$

Subscripts i, j denote spatial sites on a square lattice, and superscripts $\alpha = 1, 2$ label the two layers. We study the case when the intraplane exchange constants $J^\alpha = J$ are the same, and we choose $J = 1$ to set the energy scale. g is the interlayer exchange.

Our treatment models disorder via site removal in one of the Heisenberg layers. This is an appropriate

picture for the doping of Cd for Co, which is thought to reduce sharply the hybridization of the conduction electrons to the Ce moment. Our motivation for studying a model of localized spins is in part pragmatic. Accessible system sizes for QMC simulations of itinerant fermion systems are not sufficiently large to encompass multiple impurities and carefully study finite size effects. However, it is also known that many of the qualitative features of itinerant AF models like the Hubbard Hamiltonian are reflected in their spin counterparts¹⁴, notably the successful modeling of the Knight shift anomaly which can be captured either with descriptions in terms of localized spins¹⁵ or itinerant electrons¹⁶.

In the absence of disorder, the position of the AF-singlet transition has been located by Sandvik to high accuracy through a finite size extrapolation of the AF order parameter

$$\langle m^2 \rangle = \left\langle \left(\frac{1}{N} \sum_i (-1)^{x_i + y_i + \alpha} S_i^\alpha \right)^2 \right\rangle \quad (2)$$

For the symmetric case^{22,23}, $J^1 = J^2$, the critical interlayer exchange $g_c = 2.5220$. For the ‘Kondo-like’ lattice where one of the intralayer J is zero, $g_c = 1.3888$.

As in Ref. [22] we use the stochastic series expansion (SSE) to obtain $\langle m^2 \rangle$. SSE samples terms in a power expansion of $e^{-\beta \hat{H}}$ in the partition function, using operator loop (cluster) updates to perform the sampling efficiently²⁴. Here we consider bilayer systems with $N = 2 \times L \times L$ and L up to 100 sites.

We also evaluate the NMR relaxation rate, given by the low frequency limit of the dynamic susceptibility

$$\frac{1}{T_1} = T \lim_{\omega \rightarrow 0} \sum_q A^2 \frac{\chi''(q, \omega)}{\omega} \quad (3)$$

where A is the hyperfine coupling. We obtain $1/T_1$ using the long imaginary-time behavior of the spin-spin correlation function

$$\frac{1}{T_1} = \frac{A^2}{\pi^2 T} \langle S_i(\tau = \beta/2) S_i(\tau = 0) \rangle \quad (4)$$

The regime of validity of this expression is discussed in Ref. [25].

AF Domains and Impurity Susceptibility: The behavior of $\langle m^2 \rangle$ as a function of the fraction of removed sites, p , is shown for a range of g in Fig. 1. The results were averaged over 120 dilution realizations. As expected, impurities decrease $\langle m^2 \rangle$ deep within the AF phase ($g = 2$) where they act to reduce the average coordination number of the lattice and hence the tendency to order. Closer to the QCP, a different behavior emerges. Impurities begin to inhibit singlet formation by leaving unpaired moments on their

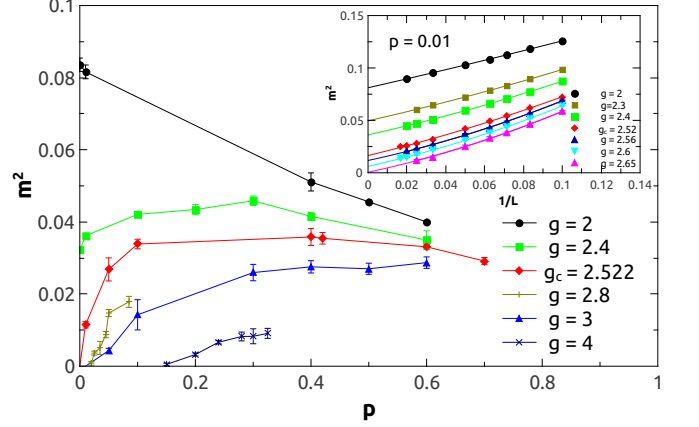


FIG. 1. The square of the staggered magnetization, $\langle m^2 \rangle$, as a function of the impurity concentration, p , for different values of g . In the AF phase with $g = 2 \ll g_c = 2.522$, impurities reduce the order. The effect of impurities near the QCP and in the singlet phase is discussed in the text. Inset: Finite size scaling of $\langle m^2 \rangle$ for $p = 0.01$. The position of the QCP is increased to $g_c(p = 0.01) = 2.65$. Data were averaged over 120 disorder realizations. The inverse temperature $\beta = 80$.

partner sites. The AF order parameter, which had been disrupted by singlet formation, therefore increases with p for $g \lesssim g_c$, and does so especially sharply at $g = g_c$. For $g > g_c$ impurity concentrations p which are sufficiently large can induce AF order even though these larger interplanar couplings would result in singlet formation in the pure case. The appearance of a finite p_c for $g > g_c$ is discussed further below.

The effect of impurities on the AF order parameter can be characterized by an ‘impurity susceptibility’

$$\chi_{\text{imp}} = \left. \frac{d \langle m^2 \rangle}{dp} \right|_{p=0}, \quad (5)$$

as shown in Fig. 2. χ_{imp} has a sharp peak at g_c . That is, the effect of the impurities is especially large close to the QCP where the system is delicately poised between two phases. Farther away from the QCP in the AF, $g \lesssim 2$, the impurity susceptibility is negative, as can be inferred from related data for the 2D Heisenberg model with site-dilution³⁸.

For $g > g_c$, impurities induce AF order in an otherwise singlet phase²⁶. We can estimate the critical impurity concentration as follows: Prior to the establishment of order, the coupling between two regions centered at sites i and j will oscillate in phase, with an amplitude which decays exponentially^{27,28}, $J_{\text{eff}} \approx J(-1)^{-|i-j+1|} \exp(-\langle l \rangle / \xi)$. Here $\langle l \rangle$ is the mean impurity separation and ξ is the correlation length in the clean system. For the 2D system considered here, $\langle l \rangle = 1/\sqrt{p}$. Assuming that the AF order will set in when the average distance between the impurities is on the same scale as ξ , yields the condition $\xi \sqrt{p_c} \approx 1$.

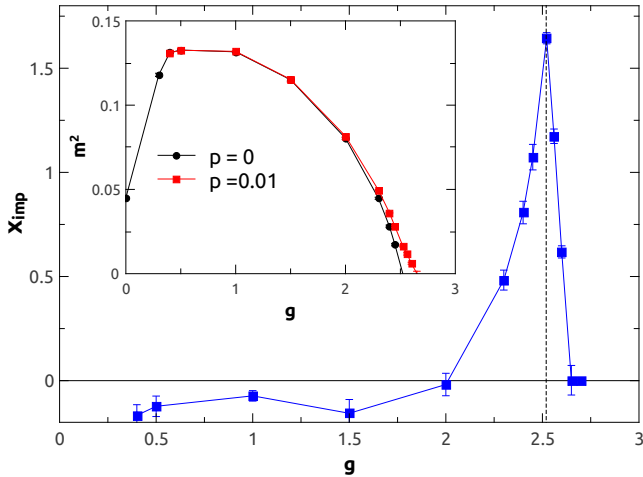


FIG. 2. The impurity susceptibility, χ_{imp} , as function of g is sharply peaked at g_c (vertical dashed line): impurities induce AF order. Away from g_c , $\chi_{\text{imp}} < 0$: impurities reduce the AF order parameter. Inset: shows the g dependence of $\langle m^2 \rangle$ for $p = 0.01$ (square) and clean system (circles). Both the shift in g_c and the large effect of impurities at the QCP are evident. Data for $\langle m^2 \rangle$ have been extrapolated to $L = \infty$. The inverse temperature $\beta = 80$.

Assuming the system is dilute, we can compute ξ by embedding a single impurity in the lattice and evaluating the decay of the spin-spin correlation in its vicinity; See Supplemental Materials. Fig. 3(a) shows the resulting ξ . The center panel validates the picture that the critical concentration of impurities to induce AF order occurs when $\langle l \rangle = 1/\sqrt{p_c} \propto \xi$.

There are several subtleties to this argument. At $T = 0$, it has been argued that an exponentially small interaction between impurities can induce order³⁰. (This occurs despite the fact that some impurity pairs, which are sufficiently close spatially, lock into singlets³¹). This suggests $p_c = 0$ throughout the singlet phase- an arbitrarily small number of impurities will order despite the rapid decay of their coupling. The effect of these very small couplings is, however, seen only at extremely low T , a fact that is reflected in SSE simulations³⁰ by the need to study inverse temperatures β as large as $\beta \sim 10^4 - 10^5$ (except very close to the QCP where ξ diverges). In contrast, β which is 2-3 orders of magnitude smaller is sufficient to reach the ground state on lattices of $L \sim 60$ studied here.

The ordering temperatures observed in Cd-doped CeCoIn5 are about 2-5 K, and the c-f coupling is reported to be around 49 meV, so that $T_c \sim 10^{-2} J$. Thus a more refined interpretation of Fig. 3(b) is that, although AF likely exists at infinitesimal p_c strictly at $T = 0$, panel (b) gives the effective critical impurity concentration to induce AF in the singlet phase at experimental temperature scales³⁹. Fig. 3(c) shows the position of the sharp cross-over which occurs in the AF order parameter at these scales.

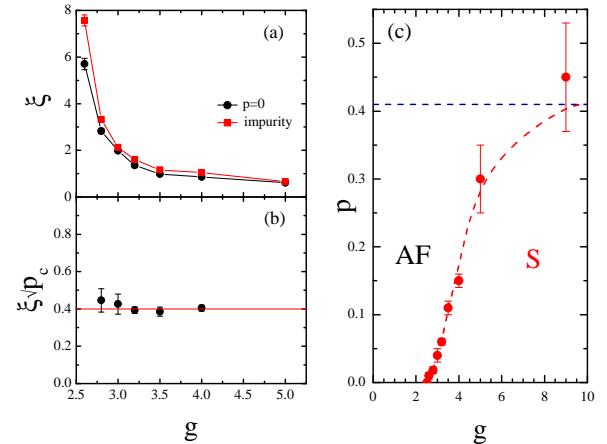


FIG. 3. (a) Correlation length ξ as function of g . Data are shown both around a single impurity (square) and for the clean system (circles). (b) $\xi\sqrt{p_c}$ as a function of g is roughly constant, consistent with a qualitative picture where AF order occurs when the mean impurity separation $\langle l \rangle$ is proportional to ξ . See text. Data for inverse temperatures $\beta = 40, 80$ were compared to ensure convergence to the ground state. L up to 100 was used to calculate ξ . (c) The AF order parameter at fixed $\beta = 80$ exhibits a sharp crossover indicating the position of the enhanced range of AF order created by the spin-1/2 impurities left behind on a fraction p of sites.

Universal Behavior of the NMR relaxation rate: The NMR spin relaxation rate, $1/T_1$ provides a crucial experimental window into doped heavy fermion materials where secondary peaks in the spectra, and broadening of the main spectral line implicate the presence of inhomogeneous environments¹³. In this section we provide a quantitative description of the effect of impurities on $1/T_1$ and demonstrate that these provide a crisp signature at the QCP, shown to higher resolution in the inset.

The main panel of Fig. 4a shows the evolution of $1/T_1$ with interlayer coupling at different fixed temperatures. $1/T_1$ follows the same trend as the AF order parameter $\langle m^2 \rangle$, i.e. it initially rises as the two planes are coupled, has a maximum for $g \approx 0.5$, and then decreases to small values at the QCP. The T independence of $1/T_1$ ^{36,37}, see the Supplemental material, is emphasized by the common crossing point at $g_c \sim 2.52$, see inset of Fig. 4a.

The behavior of $1/T_1$ in the presence of disorder is shown in Fig. 4b. We consider the most simple case where a spin is removed from one layer, and compute the relaxation rate of spins in the pure layer as a function of distance x on a horizontal line from the removed site. $x = 0$ in the figure thus corresponds to the removed spin's immediate partner, while $x = 1, 2$ are near and next-near neighbors, and, finally, at $x = L/2$, far away from the impurity. For $x = 0$ the partner spin shows a sharp signature of the QCP. Above $g = g_c$, when all the other spins are locked in singlets, the free spin-1/2

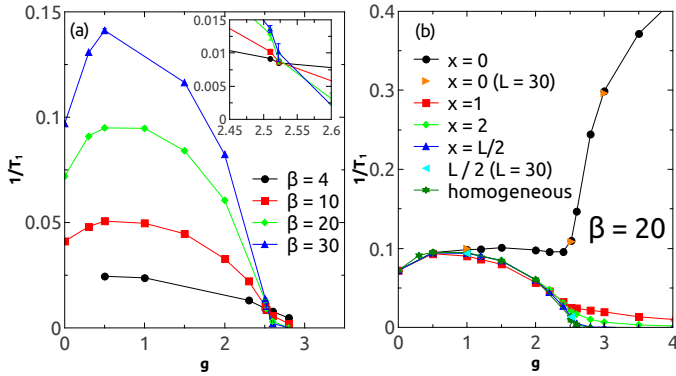


FIG. 4. (a) $1/T_1$ as a function of g for different values of β . The linear size $L = 50, 60$. Inset: Blow-up of the crossing point. $g < g_c$, $g = g_c$ and $g > g_c$. (b) g dependence of $1/T_1$ for a system with a single removed spin. $x = 0, 1, 2, L/2$ are different horizontal distances from the impurity. See text. For the impurity system the linear lattice size $L = 20, 30$.

left behind by the spin removal has a greatly enhanced $1/T_1$. Meanwhile, the relaxation rate is small for all other sites. For $g = 0$ the spins in the undiluted plane are decoupled from the second layer, and hence will all share a common value of $1/T_1$ regardless of impurities placed there. Figure 4b indicates that this independent plane behavior approximately extends out to $g \gtrsim g_c$ for $x \geq 1$. The curve for $x = 0$ breaks away for $g \geq 1$, and, as noted earlier, has a very sharp increase at the QCP. The comparison with the curve of the homogeneous system shows, as is observed experimentally³⁹, that the $1/T_1$ of the farthest spin is unaffected by the impurity. In the Supplemental Material further details on the spatial distribution of $1/T_1$ are provided.

We conclude our discussion of the relaxation rate by computing the temperature dependence of $1/T_1$ at the QCP, $g = 2.52$, for this same collection of sites. As emphasized by Fig. 5, $1/T_1$ is only weakly temperature dependent away from the impurity site. For the spin left behind at $x = 0$, $1/T_1$ increases substantially as T is lowered. The growth can be described by a power law. (See inset.) Sachdev *et. al.* have argued¹⁹ that the imaginary-time autocorrelation function of an impurity at the QCP follows the scaling form, $S_i(\tau)S_i(0) \sim \tau^{\eta'}$, which implies, (Eq. 4), that $1/T_1 \sim T^{(\eta'-1)}$. Here we obtain $\eta' = 0.41 \pm 0.03$, in agreement with Ref. [20].

Finally, in Fig. 6, we study the AF puddles which are believed to form around Cd sites, and their interactions. For $g = 4$ only spins in the close vicinity of an impurity at the lattice center are correlated with it. When $g = 3$ the locations of the other impurities become evident. Correlations starting to become substantial over the whole lattice at $g \sim 2.7$. For this density of impurities, $p = 0.01$ (16 impurities on a 40×40 lattice) finite size scaling showed that $p_c \sim 2.52$. (See inset to Fig. 1.) The enhanced values of the spin correlations at the clean system QCP (bottom right panel) are consistent

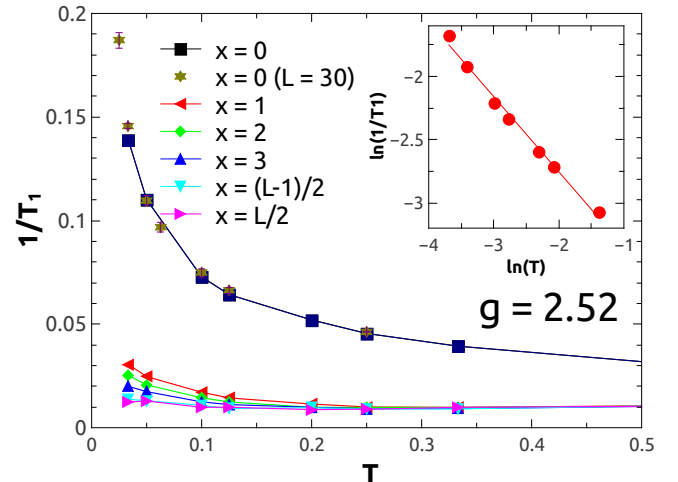


FIG. 5. T dependence of $1/T_1$ for separations x from the impurity. See text. Inset: Determination of the η' exponent. Linear lattices sizes were $L = 20, 30$, somewhat smaller than in previous figures because of the necessity to compute the imaginary time dependent correlation functions.

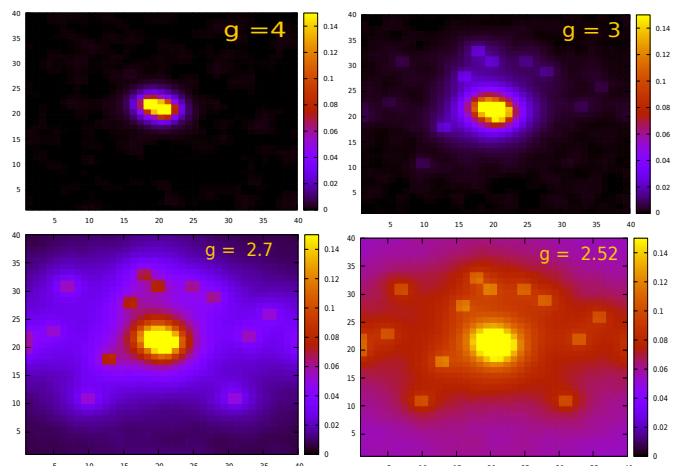


FIG. 6. Correlation of the spin at an impurity site, chosen to be at the center of the lattice, with spins at other sites. Deep in the singlet phase $g = 4$, top left, the ordered region is confined to the immediate vicinity of the site. As g decreases towards the QCP, this puddle first expands, top right, followed by the emergence of large values at the locations of the unpaired spins at other impurity sites, bottom left and right.

with the establishment of a non-zero value for the order parameter, $m^2 \sim 0.02$ in Fig. 1. Results for the puddle formed by a single impurity are in the Supplementary materials.

Conclusions and Outlook: Exploration of the effect of randomness and dilution on magnetic and superconducting order is a crucial step to understanding disordered, strongly interacting quantum systems such as heavy fermion and cuprate materials, particularly

near quantum critical points. Impurities reduce order, but can also nucleate ordered domains which, when sufficiently close to one another, can coalesce to create long range order³²⁻³⁴. In this paper we have brought together exact QMC calculations of the effect of impurities on spin correlations/domains and the nuclear magnetic resonance relaxation rate as a system is tuned through a QCP.

Our key conclusions are that: (i) the impurity susceptibility, defined as the response of the AF order parameter to the removal of a small number of spins, exhibits a sharp peak at the QCP, so that low disorder concentrations readily lead to long range order; (ii) The critical concentration p_c for randomness to induce long range AF order in the singlet phase, at moderate β , is well described by $\xi \sqrt{p_c} \sim 0.4$, where ξ is the spin correlation length at $g > g_c$; and (iii) Verification of the

suggestion that the NMR relaxation rate is temperature-independent at the QCP, and that an abrupt increase in the local value of $1/T_1$ on an impurity site provides a clear signature of the QCP.

Our work has focussed on localized Heisenberg spins. Analogous studies within itinerant electron Hamiltonians like the periodic Anderson model, are underway³⁵.

Acknowledgements: We would like to thank Rajiv Singh and Eric Andrade for very useful discussions. T.P. and R.R.S. acknowledges support from CNPq and CAPES, FAPERJ, and the INCT on Quantum Information. R.T.S. and N.C. acknowledge support from the NNSA grant DE-NA0002908. T.M., T.P. and R.T.S. acknowledge funding from Science Without Borders, Brazil. G.B. acknowledges support from Institut Universitaire de France, MajuLab, and Centre for Quantum Technologies. R.T.S. and G.B. thank T. Fratellis.

¹ “Superconductor-to-nonsuperconductor transition in $(La_{1-x}Sr_x)_2CuO_4$ as investigated by transport and magnetic measurements,” H. Takagi, T. Ido, S. Ishibashi, M. Uota, S. Uchida, and Y. Tokura, Phys. Rev. B40, 2254 (1989).

² “Optical spectra of $La_{2-x}Sr_xCuO_4$: Effect of carrier doping on the electronic structure of the CuO_2 plane,” S. Uchida, T. Ido, H. Takagi, T. Arima, Y. Tokura, and S. Tajima, Phys. Rev. B43, 7942 (1991).

³ “High-temperature superconductivity in tetragonal perovskite structures: Is oxygen-vacancy order important?”, Gang Xiao, M. Z. Cieplak, A. Gavrin, F. H. Streitz, A. Bakhshai, and C. L. Chien, Phys. Rev. Lett. 60, 1446 (1988).

⁴ “Néel transition and sublattice magnetization of pure and doped La_2CuO_4 ”, B. Keimer, A. Aharony, A. Auerbach, R. J. Birgeneau, A. Cassanho, Y. Endoh, R. W. Erwin, M. A. Kastner, and G. Shirane, Phys. Rev. B45, 7430 (1992).

⁵ “⁸⁹NMR probe of Zn induced local moments in $YBa_2(Cu_{1-y}Zn_y)_3O_{6+x}$ ”, A. V. Mahajan, H. Alloul, G. Collin, and J. F. Marucco, Phys. Rev. Lett. 72, 3100 (1994).

⁶ “Optical study of the $La_{2-x}Sr_xNiO_4$ system: Effect of hole doping on the electronic structure of the NiO_2 plane,” T. Ido, K. Magoshi, H. Eisaki, and S. Uchida, Phys. Rev. B44, 12094(R) (1991).

⁷ “Electron and hole doping in NiO ,” F. Reinert, P. Steiner, S. Hüfner, H. Schmitt, J. Fink, M. Knupfer, P. Sandl, and E. Bertel, Z. Phys. B97, 83 (1995).

⁸ “Spin-Peierls and antiferromagnetic phases in $Cu_{1-x}Zn_xGeO_3$: A neutron-scattering study”, Michael C. Martin, M. Hase, K. Hirota, G. Shirane, Y. Sasago, N. Koide, and K. Uchinokura, Phys. Rev. B56, 3173 (1997).

⁹ “Switching of the gapped singlet spin-liquid state to an antiferromagnetically ordered state in $Sr(Cu_{1-x}Zn_x)_2O_3$,” M. Azuma, Y. Fujishiro, M. Takano, M. Nohara, and H. Takagi, Phys. Rev. B55, R8658 (1997).

¹⁰ “Disorder and Impurities in Hubbard Antiferromagnets”, M. Ulmke, P. J. H. Denteneer, V. Janis, R. T. Scalettar, A. Singh, D. Vollhardt, and G. T. Zimanyi, Adv. Sol. St. Phys. 38, 369 (1999).

¹¹ “Impurity effects at finite temperature in the two-dimensional $S = 1/2$ Heisenberg antiferromagnet,” K.H. Hoglund and A.W. Sandvik, Phys. Rev. B70, 024406 (2004).

¹² “Reversible tuning of the heavy-fermion ground state in $CeCoIn_5$ ”, L.D. Pham, T. Park, S. Maquilon, J.D. Thompson, and Z. Fisk, Phys. Rev. Lett. 97, 056404 (2006).

¹³ “Disorder in quantum critical superconductors,” S. Seo, Xin Lu, J.-X. Zhu, R.R. Urbano, N. Curro, E.D. Bauer, V.A. Sidorov, L.D. Pham, Tuson Park, Z. Fisk and J.D. Thompson, Nature Physics 10, 120 (2014).

¹⁴ In fact, bilayer Hubbard and Heisenberg models can even track each other semi-quantitatively. For example, the Hubbard QCP $(t_\perp/t)_c \sim 1.6$ is rather close to that obtained from the Heisenberg limit $(J_\perp/J)_c = 2.522$ assuming $J = 4t^2/U$. See ‘Magnetic and Pairing Correlations in Coupled Hubbard Planes.’ R.T. Scalettar, J.W. Cannon, D.J. Scalapino, and R.L. Sugar, Phys. Rev. B50, 13419 (1994).

¹⁵ “Long range order and two-fluid behavior in heavy electron materials,” K.R. Shirer, A.C. Shockley, A.P. Dioguardi, J. Crocker, C.-H. Lin, N. apRoberts-Warren, D. M. Nisson, P. Klavins, J.C. Cooley, Y.-F. Yang, and N. J. Curro, Proc. Nat. Acad. Sci. 109, 18249 (2012).

¹⁶ “Universal Knight shift anomaly in the Periodic Anderson model”, M. Jiang, N.J. Curro, and R.T. Scalettar, Phys. Rev. B90, 241109 (2014).

¹⁷ “Similarities between the Hubbard and Periodic Anderson Models at Finite Temperatures”, K. Held, C. Huscroft, R.T. Scalettar, and A.K. McMahan, Phys. Rev. Lett. 85, 373 (2000).

¹⁸ “Multicritical point in a Diluted Bilayer Heisenberg Quantum Antiferromagnet,” A.W. Sandvik, Phys. Rev. Lett. 89, 177201 (2002).

¹⁹ “Quantum impurity in a nearly-critical two dimensional antiferromagnet,” S. Sachdev, C. Buragohain, and M.

Vojta, Science 286, 2479 (1999).

²⁰ “Impurity Induced Spin Texture in Quantum Critical 2D Antiferromagnets,” K.H. Höglund, A.W. Sandvik, and S. Sachdev, Phys. Rev. Lett. 98, 087203 (2007).

²¹ “Site-dilution-induced antiferromagnetic long-range order in a two-dimensional spin-gapped Heisenberg antiferromagnet,” C. Yasuda, S. Todo, M. Matsumoto, and H. Takayama, Phys. Rev. B64, 092405 (2001).

²² “Order-disorder transition in a two-layer quantum antiferromagnet,” A.W. Sandvik and D.J. Scalapino, Phys. Rev. Lett. 72, 2777 (1994).

²³ “High-precision finite-size scaling analysis of the quantum critical point of $S = 1/2$ Heisenberg antiferromagnetic bilayers”, L. Wang, K.S.D. Beach, and A.W. Sandvik, Phys. Rev. B73, 014421 (2006).

²⁴ “Quantum Monte Carlo with Directed Loops”, O.F. Syljuasen and A. W. Sandvik, Phys. Rev. E66, 046701 (2002).

²⁵ “Pairing and Spin Gap in the Normal State of Short Coherence Length Superconductors”, M. Randeria, N. Trivedi, A. Moreo, and R.T. Scalettar, Phys. Rev. Lett. 69, 2001 (1992).

²⁶ “Nonmagnetic impurities in spin-gapped and gapless Heisenberg antiferromagnets”, A. W. Sandvik, E. Dagotto, and D. J. Scalapino, Phys. Rev. B56, 11701 (1997).

²⁷ “Low-Temperature Properties of the Randomly Depleted Heisenberg Ladder”, M. Sigrist and A. Furusaki, J. Phys. Soc. Jpn. 65, 2385 (1996)

²⁸ “Order by Disorder from Nonmagnetic Impurities in a Two-Dimensional Quantum Spin Liquid”, Stefan Wessel, B. Normand, M. Sigrist, and S. Haas, Phys. Rev. Lett. 86, 1086 (2001).

²⁹ “Impurity-Induced Magnetic Order in Low-Dimensional Spin-Gapped Materials”, J. Bobroff, N. Laflorencie, L. K. Alexander, A.V. Mahajan, B. Koteswararao, and P. Mendels, Phys. Rev. Lett. 103, 047201 (2009).

³⁰ “Magnetic ordering in a doped frustrated spin-Peierls system,” N. Laflorencie, D. Poilblanc, and A.W. Sandvik, Phys. Rev. B69, 212412 (2004).

³¹ “Field-induced quantum-disordered phases in $S = 1/2$ weakly coupled dimer systems with site dilution,” T. Roscilde, Phys. Rev. B74, 144418 (2006).

³² “Local defect in metallic quantum critical systems,” A.J. Millis, D.K. Morr, and J. Schmalian, Phys. Rev. Lett. 87, 167202 (2001).

³³ “Spin and charge order around vortices and impurities in high- T_c superconductors,” J-X. Zhu, I. Martin, and A.R. Bishop, Phys. Rev. Lett. 89, 067003 (2002).

³⁴ “Disorder-induced static antiferromagnetism in cuprate superconductors,” B.M. Andersen, P.J. Hirschfeld, A.P. Kampf, and M. Schmid, Phys. Rev. Lett. 99, 147002 (2007).

³⁵ “Impurity-Induced Antiferromagnetic Domains in the Periodic Anderson Model,” A. Benali, Z. Bai, N.J. Curro, and R.T. Scalettar, arXiv:1604.02735.

³⁶ “Universal Magnetic Properties of $\text{La}_{2-\delta}\text{Sr}_\delta\text{CuO}_4$ at Intermediate Temperatures” A.V. Chubukov and S. Sachdev, Phys. Rev. Lett. 71, 169 (1993).

³⁷ “Locally critical quantum phase transitions in strongly correlated metals” Q. Si, S. Rabello, K. Ingersent, and J.L. Smith, Nature 413, 804 (2001).

³⁸ “Classical percolation transition in the diluted two-dimensional $S = 1/2$ Heisenberg antiferromagnet” A.W. Sandvik, Phys. Rev. B 66, 024418 (2002).

³⁹ “Interacting Antiferromagnetism Droplets in Quantum Critical CeCoIn_5 ” R.R. Urbano *et. al.*, Phys. Rev. Lett. 99, 146402 (2007).

Supplementary Material: At the QCP, Fig. (1) of the main text showed that $\langle m^2 \rangle$ is significantly different from zero even for a small fraction of impurities, $p = 0.01$. In Fig. S1 we provide further details by showing the staggered correlation function, $C(r) = (-1)^{(i+r)} S_i^1 S_{i+r}^1$, of a single impurity at $g = g_c$. Here S_i^1 is the spin in layer 1 left without a partner by the dilution at site i . $C(r)$ is enhanced around such a “lonely site”, in comparison with $C(r)$ in the clean system (also shown).

The log-log plot in the inset shows the decay is power law. In the clean system, $C(r) \sim 1/r^{1+\eta}$, where $\eta = 0.03$ is the 3D Heisenberg model critical exponent. The impurity $C(r)$ also follows a power law decay, but with an exponent $\alpha \approx 0.67 \pm 0.02 < 1 + \eta$. For $g > g_c$ the singlet gap opens and $C(r)$ decays exponentially, as discussed in the main text.

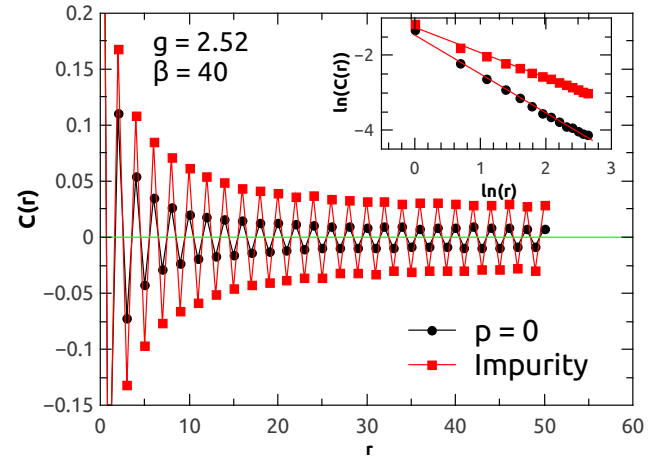


FIG. S1. Staggered spin correlation function, $C(r)$, at $g = g_c$ for a single impurity (square) and clean system (circle). **Inset:** Power law behavior of $C(r)$. A stronger AF cloud is produced about the unpaired impurity moment.

Fig. (6) of the main text showed the AF clouds around a collection of impurities for various depths into the singlet phase. Here Fig. S2 illustrates the cloud produced by a single impurity. The line graph of Fig. S1 corresponds to a horizontal cut of the bottom right panel of Fig. S2.

In Fig. (S3), we re-display the data of Fig. (5), showing now $1/T_1$ as a function of temperature T . In the AF phase ($g < g_c$), $1/T_1$ increases for low T . On the other hand, due to the presence of the spin gap, $1/T_1$ goes to zero in the singlet phase ($g > g_c$). At the QCP, $g = g_c$, $1/T_1$ is almost constant for the range of temperature considered^{36,37}. This is an alternate view of the crossing of the curves of $1/T_1$ versus g shown in Fig. (4)a.

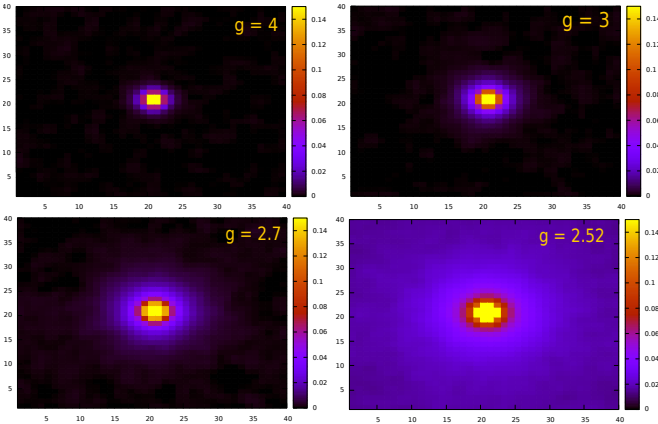


FIG. S2. Color contour plot of the AFM cloud around a *single* impurity. Deep in the singlet phase, $g = 4$ (upper left) spin correlations extend for only a few lattice spacings. This distance grows as g approaches g_c from above.

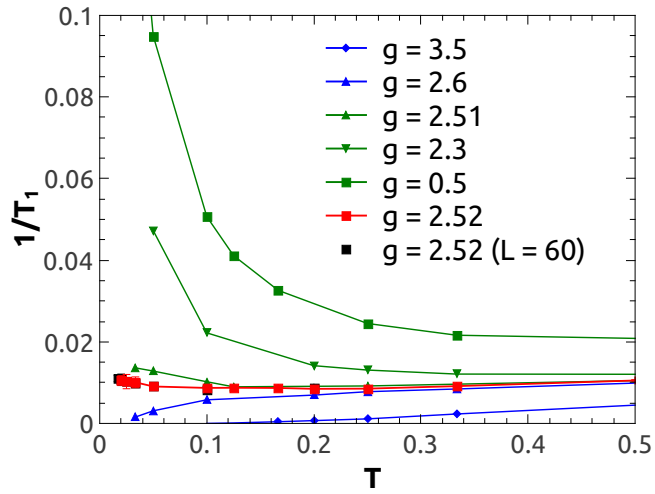


FIG. S3. $1/T_1$ as a function of T for different values of g in the homogeneous system. Linear size of the system 50, 60. At the QCP, $g = 2.52$, the relaxation rate is nearly constant.